DE GRUYTER

Chemical Papers 69 (4) 569–579 (2015)
DOI: 10.1515/chempap-2015-0065

ORIGINAL PAPER

Structural and thermal characterization of copper(II) complexes with phenyl-2-pyridylketoxime and deposition of thin films by spin coating

[a]Robert Szczęsny*, [a]Tadeusz M. Muzioł, [b]Duncan H. Gregory, [a]Edward Szłyk

[a] *Faculty of Chemistry, Nicolaus Copernicus University, 87-100 Toruń, Poland*

[b] *WestCHEM, School of Chemistry, University of Glasgow, Glasgow, G12 8QQ, UK*

Received 15 July 2014; Revised 21 August 2014; Accepted 22 August 2014

Four copper(II) oxime complexes, [Cu(HPPK)(PPK)X] (HPPK = phenyl-2-pyridylketoxime and X = Cl^- (*I*), CF_3COO^- (*II*), $C_3F_7COO^-$ (*III*), and $[Cu(PPK)_2]_2$ (*IV*)), were synthesized and characterized by elemental analysis, infrared spectroscopy (IR), and single-crystal X-ray diffraction (XRD). XRD analysis revealed that *I*–*III* contain copper(II) coordinated by four nitrogen atoms from two oxime molecules in the basal plane and one monodentate anion X in the apical position of a distorted square pyramid. Complex *IV* is dimeric and it is formed by two $Cu(PPK)_2$ units. Bridges between these units are formed by the two oxygen atoms of the deprotonated oxime groups. Thermal stability of *I*–*IV* was investigated by thermogravimetric analysis (TGA) in air and in nitrogen atmosphere, respectively. Evolved gaseous decomposition products were characterized by IR. *I*–*IV* decompose via multistep processes. Fluorocarbons and CO_2 were observed to be the most abundant gaseous species evolved. Preliminary ammonolysis experiments were performed to examine the possibility of using *II* and *IV* as precursors for the synthesis of copper nitride. Moreover, solutions of *IV* were spin-coated onto silicon substrates. Surface structure and morphology of the resulting films were studied by scanning electron microscopy (SEM) and atomic force microscopy (AFM) and layers with island-like distribution of material were observed.

Keywords: copper(II) complexes, phenyl-2-pyridylketoxime, spin coating, thermal properties, ammonolysis

Introduction

Chemistry of copper and other transition metal pyridine oximes has been long investigated considering their application as analytical reagents (Meek & Chene, 1965). Currently, however, there is a renewed interest in the chemistry of oximes given the many possibilities of their application such as new oxygen activation catalysts, corrosion inhibitors, building blocks in the design of homo- and heterometallic clusters and coordination polymers, etc. (Milios et al., 2004, 2006; Afrati et al., 2010). In the transition metal complexes of neutral 2-pyridyl ketoxime, the nitrogen atom of the oxime group and the nitrogen atom of the HPPK pyridyl group can bind in the *N*,*N*′-chelating mode. Also, HPPK is a potential ambidentate ligand, in which coordination is also possible via the oxygen atom. Importantly, oximes are weak acids and so the type of the metal-binding depends on pH. HPPK can bind to metals as either a neutral (HL) and/or a deprotonated (L) ligand (Salonen et al., 2003; Chakravorty, 1974) yielding, for example, trinuclear clusters with copper characterized as the inverse of 9-metallacrown-3 (Liu et al., 2010; Afrati et al., 2007). Surprisingly, despite all that is known regarding complexes formed with copper(II) and HPPK, crystal structures of these compounds are seldom found. Excluding metallacrown systems, to the best of our

*Corresponding author, e-mail: roszcz@umk.pl

knowledge, there are only two known Cu(II)–HPPK crystal structures: $[Cu_2Cl_4(HPPK)_2]$ (Li et al., 2006) and $[Cu_2(hfac)_2(PPK)_2]$ (Koumousi et al., 2010). Similarly, although the thermolysis of various types of transition metal oxime complexes is known (Hudák & Košturiak, 1999; Prathapachandra Kurup et al., 2000) no studies on the thermal behavior of Cu(II)–HPPK complexes were published.

Therefore, the principal purpose of our study is to identify the crystal structures of copper(II)–HPPK complexes in combination with different anions exhibiting flexible binding modes and to examine their thermal properties. Having fully characterized the compounds, our intention was to investigate the application of these complexes as precursors in spin coating processes (SC), which is an efficient method to grow polymeric (Hall et al., 1998), inorganic (Partridge et al., 1996; Sathaye et al., 2003), and metallic (Kim et al., 2008) thin films with easily controlled coating coverage (Schubert & Dunkel, 2003). Moreover, the technique can also be employed to deposit layers of transition metal complexes with interesting magnetic, optical, or catalytic properties (Bräuer et al., 2006; Elschner et al., 2001).

The idea was to take advantage of the good solubility of copper(II)–HPPK complexes and examine them as potential precursors for facile low cost fabrication of semiconducting thin films (e.g., CuO, Cu_2O, and Cu_3N). Moreover, these oximes have the ability to form hetero-bimetallic chelates, which makes them potential candidates for the preparation of mixed metal semiconductors with a prescribed molar ratio (Liu & Liu, 1961). Cu_2O and CuO are stable p-type semiconductors and a variety of methods have been used to fabricate thin films of copper oxides (Barreca et al., 2009; Bayansal et al., 2012). Copper nitride, Cu_3N, meanwhile, has been proposed for the use in optical storage (Ji et al., 2006) and as a component of spintronic systems (Navío et al., 2009). There are several examples of copper oxide film fabrication by SC in literature. They can be formed by CuO or Cu_2O synthesis, e.g. by sol–gel processing (Baker et al., 2007) in the initial step followed by the deposition (Kida et al., 2007) or by precursor deposition followed by annealing in air. In the latter case, copper acetate (Huh et al., 2012) or naphthenate (Ando et al., 2003) were used as precursors. Thin films of Cu_3N have been produced almost exclusively by physical techniques such as magnetron sputtering (Wang et al., 2006).

Thermal decomposition of copper oximes in nitrogen or air is investigated as a potential route leading to Cu_2O or CuO film production. Moreover, reported experiments on the Cu_3N synthesis, prompted us to react HPPK complexes with gaseous NH_3 to determine if ammonolysis can be exploited to prepare films of copper nitride (Paniconi et al., 2007). It has been proved that phase-pure CuO can be obtained in air and thus, after preliminary coating experiments for complex *IV,* samples were heated in air and film morphology was analyzed by the SEM and AFM techniques.

Experimental

All materials and solvents were purchased commercially (Aldrich, POCh, Gliwice, Poland) and used without further purification. Thermal studies (TG, DTG, DTA) were performed using a TA SDT 2960 analyzer (TA Instruments, New Castle, DE, USA). Decomposition processes were studied in dynamic atmosphere of dry nitrogen and air, respectively, at the flow rate of 40 mL min^{-1} and under heating to 1000 ℃ at 10 ℃ min^{-1}. Gaseous decomposition products were detected by an FT IR FTS-3000 Excalibur spectrophotometer (BioRad, Hercules, CA, USA) coupled with the TA SDT 2960 analyzer. SEM studies were performed on a LEO 1430 VP (Cambridge, UK) microscope equipped with a Quantax 200 (XFlash 4010 detector, Bruker AXS, Karlsruhe, Germany) EDX spectrometer. AFM imaging was performed using a NanoScope MultiMode SPM System (Veeco-Digital Instrument, San Diego, CA, USA). IR spectra of *I*–*IV* were collected with a Perkin–Elmer (Waltham, MA, USA) 2000 FT IR spectrometer in the range of 4000–400 cm^{-1} using KBr discs. Powder X-ray diffraction (PXD) analysis was performed using a Philips (Almelo, The Netherlands) XPERT θ–2θ diffractometer with CuK_α radiation.

Complex $[Cu(HPPK)(PPK)Cl]\cdot H_2O$ (*I*) was prepared as reported by Meek and Chene (1965) by the reaction of copper(II) chloride dihydrate with phenyl-2-pyridylketoxime. The $C_{24}H_{21}ClCuN_4O_3$ composition (w_i (mass %)) was: calc. C 56.3, H 4.1, N 10.9; found C 56.1, H 4.0, N 10.5. IR ($\tilde{\nu}$ (cm^{-1})): 3435 ν(C═N)$_{pyridyl}$; 1598, 1466, 1105, 1024 ν(N—O); 975, 705.

Compounds $[Cu(HPPK)(PPK)(CF_3COO)]$ (*II*) and $[Cu(HPPK)(PPK)(C_3F_7COO)]$ (*III*) were prepared by a similar method. Complex *I* (0.082 g, 0.16 mmol) was dissolved in a small amount of a water–ethanol solution (10 : 1). Then, CF_3COOAg (0.035 g, 0.16 mmol, for *II*) or C_3F_7COOAg (0.051 g, 0.16 mmol, for *III*) were added. The white AgCl precipitate formed was filtered and the green solution was dried in air and then in vacuo. The $C_{26}H_{19}CuF_3N_4O_4$ (*II*) composition (w_i (mass %)) was: calc. C 54.6, H 3.3, N 9.8; found C 54.4, H 3.9, N 9.3. IR ($\tilde{\nu}$ (cm^{-1})): 3448 ν_{as}(COO); 1678 ν(C═N)$_{pyridyl}$; 1597, 1472, 1133 ν(N—O); 975, 704. The $C_{28}H_{19}CuF_7N_4O_4$ (*III*) composition (w_i (mass %)) was: calc. C 50.0, H 2.8, N 8.3, found C 49.8, H 2.9, N 8.6. IR ($\tilde{\nu}$ (cm^{-1})): 3448 ν_{as}(COO); 1698 ν(C═N)$_{pyridyl}$; 1595, 1469, 1214, 1116 ν(N—O); 964, 704.

Complex $[Cu(PPK)_2]_2\cdot 3.4H_2O$ (*IV*) was prepared as follows: cupric carboxylate $(CH_3CH_2C(CH_3)_2COO)_2Cu$ (0.099 g, 0.34 mmol) was dissolved in

Table 1. Crystal data and structure refinement for *I–IV*

Characterization data	*I*	*II*	*III*	*IV*
Empirical formula	$C_{24}H_{21}ClCuN_4O_3$	$C_{26}H_{19}CuF_3N_4O_4$	$C_{28}H_{19}CuF_7N_4O_4$	$C_{24}H_{25.4}0CuN_4O_{3.70}$
Formula mass	512.44	571.99	672.02	492.62
Crystal system	monoclinic	monoclinic	monoclinic	monoclinic
Space group	P 2(1)/n	P 2(1)/c	C 2/c	C 2/c
a (Å)	9.1844(3)	9.1653(3)	26.798(5)	26.832(3)
b (Å)	13.7589(5)	17.4582(4)	8.735(5)	11.5169(6)
c (Å)	18.0176(6)	15.5793(4)	22.803(5)	17.519(2)
α (°)	90.00	90.00	90.00	90.00
β (°)	91.558(3)	97.282(2)	95.343(5)	125.83(2)
γ (°)	90.00	90.00	90.00	90.00
Volume (Å^3)	2276.00(13)	2472.74(11)	5315(3)	4389.4(9)
Z	4	4	4	8
D_{calc} (Mg m^{-3})	1.495	1.536	1.680	1.491
μ (mm^{-1})	1.111	0.947	0.916	1.033
Crystal size (mm)	0.45 × 0.39 × 0.16	0.31 × 0.12 × 0.08	0.34 × 0.20 × 0.06	0.31 × 0.09 × 0.02
Temperature (K)	293(2)	293(2)	293(2)	293(2)
Reflections collected	8106	15447	9379	6834
Independent reflections/Rint	4660/0.0367	5064/0.0885	4688/0.1072	3777/0.0629
Max. and min. transmission	0.8422/0.6347	0.6403/0.2529	0.9471/0.7460	0.9796/0.7400
Goodness-of-fit on F^2	0.959	1.007	0.810	0.826
R_1 $[I > 2\alpha(I)]$	0.0305	0.0447	0.0561	0.0438
wR_2 $[I > 2\alpha(I)]$	0.0822	0.1170	0.0876	0.0823
Largest diff. peak and hole (e Å^{-3})	0.315/–0.466	0.483/–0.534	0.319/–0.537	0.310/–0.368

100 mL of an ethanol–water solution (3 : 1). Phenyl-2-pyridylketoxime (0.134 g, 0.68 mmol) was added and the resulting dark red-brown precipitate was allowed to stand overnight before drying in vacuo. The $C_{24}H_{25.4}CuN_4O_3$ composition (w_i (mass %)) was: calc. C 58.5 H, 5.2 N, 11.4, found C 60.94, H 4.4, N 11.7. IR ($\tilde{\nu}$ (cm^{-1})): ν(C═N)$_{pyridyl}$; 1595, 1462, 1121, 1024 ν(N—O); 973, 708.

Diffraction data of the prepared complexes were collected using an Oxford (Abingdon, UK) Sapphire CCD diffractometer with MoK_α radiation (λ = 0.71073 Å). The reflections were measured using the ω–2θ method. A numerical absorption correction was applied for the studied crystals (RED171 program package, Oxford Diffraction (2000)). Structures were solved by direct methods and refined using a full-matrix least-squares procedure on F2 (SHELX-97, Sheldrick (2008)). Heavy atoms were refined using anisotropic displacement parameters. All hydrogen atoms attached to carbon atoms were assigned to calculated positions and they were refined as riding atoms with isotropic thermal parameters fixed to a value by 20 % higher than those of the corresponding atoms to which they were bound. All structure representations were prepared in DIAMOND (Brandenburg, 2001) and ORTEP-3 (Farrugia, 1997). The results of the data collections and refinements are summarized in Table 1. CCDC 793049, 793050, 837356, and 837355 contain the supplementary crystallographic data for this paper.

Spin coated films of *IV* were deposited onto 1 cm × 1 cm × 1 mm silicon substrates. A saturated solution of *IV* in acetonitrile–methanol (1 : 6) was spun onto the substrate at 1000–5000 min^{-1} for 30–120 s and each plate was subsequently dried at the rotation speed of 5000 min^{-1} for 20 s. The coatings were then dried under vacuum for 1 h. Copper(II) oxide films were formed by heating the plates in air at 800 ℃ for 1 h. Ammonolysis reactions were performed in a horizontal tube furnace under the flow of NH_3 (BOC, Guildford, UK; 99.98 %, flow rate: 50–150 mL min^{-1}). Reactions were performed at 250–450 ℃ for 45 min to 240 min. All ammonolysis samples were cooled under NH_3 to room temperature before switching to the nitrogen gas flow (for approximately 30 min) prior to sample removal.

Results and discussion

Synthesis and characterization of complexes

Complex $[Cu(HPPK)(PPK)Cl]\cdot H_2O$ was prepared according to a literature procedure and it was used as the starting material for the synthesis of a variety of anionic compounds containing the $[Cu(HPPK)(PPK)]^+$ unit. New complexes were obtained by the reaction of *I* with appropriate silver carboxylates resulting in AgCl and dark green solutions. After the filtration and evaporation of solvents, stable crystals highly soluble in both organic solvents and water were formed.

IR spectra of all compounds contain the ν(C═N)$_{pyridyl}$ (Afrati et al., 2010) and ν(N—O) bands slightly shifted towards higher frequencies as compared to the values for the free ligand (1591 cm^{-1} and 948 cm^{-1}) (Mohan & Paramhans, 1980). The

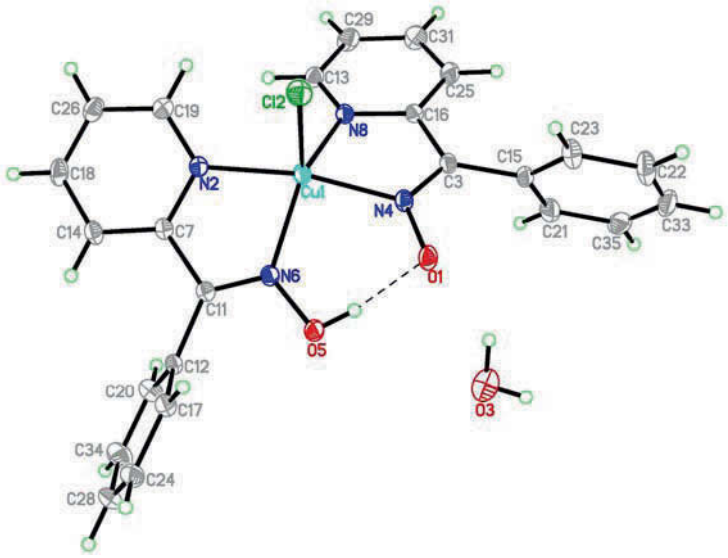

Fig. 1. Structure of $[Cu(HPPK)(PPK)Cl] \cdot H_2O$ (*I*) with thermal ellipsoids at the 20 % probability level.

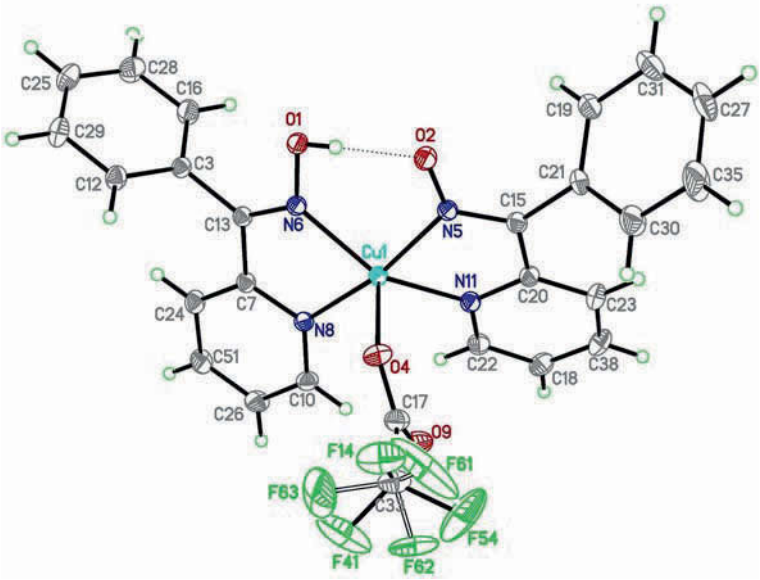

Fig. 2. Structure of $[Cu(HPPK)(PPK)(CF_3COO)]$ (*II*) with atoms numbered appropriately. Thermal ellipsoids presented are at the 20 % probability level.

acyclic ν(C═N) band from the oxime group occurs at 1628 cm^{-1} but after the coordination, the intensity and resolution of the vibration prevented its unambiguous assignment.

The monomeric complexes, $[Cu(HPPK)(PPK)Cl] \cdot H_2O$, $[Cu(HPPK)(PPK)(CF_3COO)]$, and $[Cu(HPPK)(PPK)(C_3F_7COO)]$, crystallized in the monoclinic $P2_1/n$, $P2_1/c$, and $C2/c$ space groups, respectively, with the whole molecule given by the formula in the asymmetric unit. Details of the data collection and refinement are given in Table 1. Bond lengths and angles for *I*–*III* are listed in Supplementary data.

In these three complexes, the Cu(II) ion is found in an approximately square pyramidal, five-coordinate environment. Two HPPK ligands provide four nitrogen donors in the basal plane of the polyhedron and a chlorine (*I*, Fig. 1) or an oxygen atom (*II* and *III*, Fig. 2 and Supplementary data) is located in the apical position. Angles in *I* are in the range of 79.08(6) –101.46(7)°, with two higher values: 166.96(7)° and 141.33(7)°, whereas the Cl2—Cu1—N angles are in the range from 96.11(5)° to 114.09(6)° revealing significant distortion of the polyhedron towards the trigonal bipyramidal geometry. Slightly smaller distortions were observed for *II* and *III*. The trigonality index (τ) indicates a distortion from the ideal square pyramidal environment (Addison et al., 1984). The values of τ, 0.43, 0.32, and 0.31 for *I*, *II*, and *III*, respectively, indicate that the Cu(II) ion adopts distorted square pyramidal geometry in all compounds but this distor-

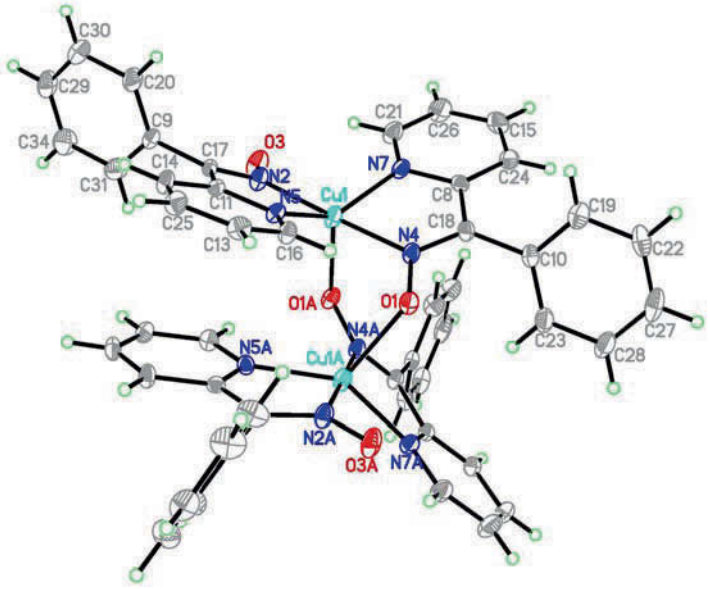

Fig. 3. Structure of $[Cu(PPK)_2]_2 \cdot 3.4H_2O$ (*IV*) with thermal ellipsoids at the 20 % probability level.

tion decreases for *I*–*III* (given that $\tau = 0$ for a square based pyramid).

In *I*–*III*, the Cu—N bond lengths were found in the range from 1.9710(16)–2.0671(17) Å, whereas in *II* they varied from 1.9740(18)–2.0434(19) Å and in *III* from 1.978(4)–2.099(4) Å. Axial ligands were bound at 2.3753(6) Å (Cu—Cl) for *I*, and at 2.1497(17) Å and 2.089(3) Å (Cu—O) for *II* and *III*, respectively. In *I*, the Cu—Cl distance is greater than the Cu—N bonds in the base of the square pyramid as expected. For *II*, however, the elongation of the Cu—O bond is rather caused by the Jahn–Teller effect. In case of *III*, the Cu—O bond distance falls within the range of the Cu—N bonds and the anticipated Jahn–Teller distortion is not evident. The differences between *II* and *III* are probably due to the similarity of the apical ligands. In *II* and *III*, the Cu(II) ion is shifted by 0.33 Å and 0.32 Å from the basal plane towards the axial O4 and O2 atoms, respectively. Phenyl rings in the HPPK or PPK moieties show distinct orientation towards the pyridyl rings. In *II*, these rings are nearly perpendicular (79.39°) for the protonated ligand, whereas they are tilted at an angle of 66.88° (similar angles are found in *III*) for the deprotonated ligand. In *I*, phenyl rings form angles of 63.63° and 72.47° to the corresponding pyridyl rings and they are closer to the values observed in *II* than to those in *III*. The dihedral angle between the HPPK phenyl rings from separate moieties is 81.75°, 66.59°, and 73.19° for *I*, *II*, and *III*, respectively, and the aromatic rings are flat within the maximal root-mean-square deviation of 0.012 Å, 0.010 Å, and 0.014 Å for *I*, *II*, and *III*, respectively. In these monomeric compounds, hydrogen is shared between the oxygen atoms from both oxime units forming very strong hydrogen bonds with the O—H bond length close to 0.82 Å (0.803–0.892) Å, H···O distance ranging from 1.570 Å in *III* to 1.669 Å in *II* and the O—H···O angle from 162.08° for *III* to 167.96° for *I*.

The $[Cu(PPK)_2]_2 \cdot 3.4H_2O$ dimer crystallized in the monoclinic C2/c space group with half of the molecule given by the formula in the asymmetric unit and all atoms in general positions (Table 1). Bond lengths and angles for *IV* are listed in Supplementary data.

The Cu(II) ion is found in an environment that can be regarded as a significantly distorted trigonal bipyramid as manifested by the τ parameter (0.59), with N2 and N4 atoms from two PPK anions in the apical positions (Fig. 3). Bond angles in the copper polyhedra reveal significant distortion of the trigonal bipyramid towards the square pyramidal geometry. Both PPK anions are deprotonated but in one of them, oxygen (O3) does not participate in the coordination. Hence, these anions are chemically and crystallographically distinct. N5 pyridyl rings (inclined only by 10°) of the two non-coordinating O3 PPK anions create strong stacking interactions inside one dimer. Cu—N bond lengths range from 1.962(3) Å to 2.041(3) Å with extreme values for the N2 and N7 atoms, respectively. Hence, bonds to the pyridyl nitrogen atoms are significantly elongated (by approximately 0.06 Å). Oxygen originating from the second half of the dimer completes the copper coordination sphere. The Cu—O1 bond (2.186(3) Å) is by ca 9 % longer than the Cu—N bonds in the base of the square pyramid, indicating the occurrence of the Jahn–Teller distortion as observed in *II*. Both phenyl rings are slightly inclined (17.42°), revealing a completely different orientation compared to that in the monomeric species, with significantly tilted (almost perpendicular) phenyl rings. The phenyl rings form angles of 67.69° and 65.01° to

Table 2. Results of the thermal analysis of *I*–*IV* in air (10 °C min^{-1})

Compound	Heat effect on DTA	Temperature[a] (°C)			Mass loss (%)	
		T_i	T_m	T_f	Calc. (for CuO formation)	Found
I	endo	67	117	156	84.5	84.3
	exo	156	174	181		
	exo	181	203	385		
	exo	385	619	663		
II	exo	168	200/205	–	86.1	83.0
	exo	–	242	–		
	exo	–	326	–		
	exo	–	440	489		
III	exo	153	175	–	88.2	87.9
	exo	–	183	–		
	exo	–	192	–		
	exo	–	318	–		
	exo	–	421	451		
IV	exo	20	55	65	83.9	91.3
	endo	165	185	–		
	exo	–	339	371		
	exo	371	448	539		

a) T_i, T_m, and T_f represent initial, at peak maximum, and final temperature, respectively.

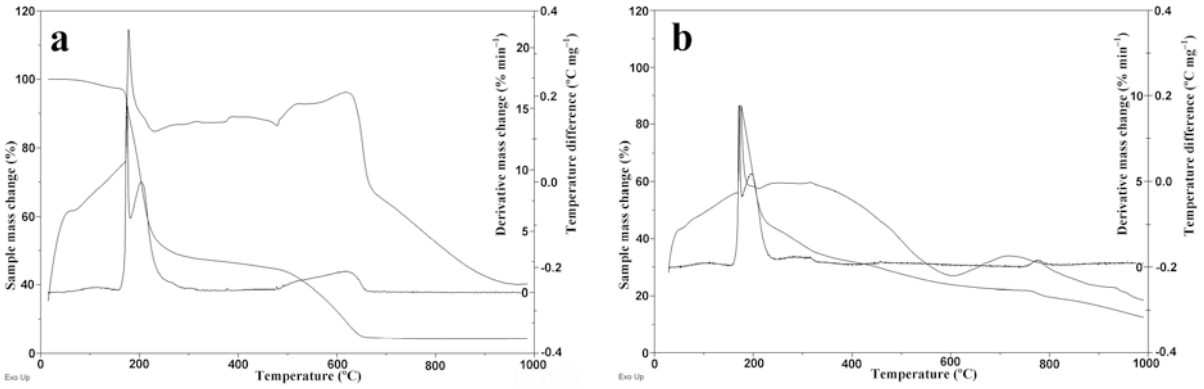

Fig. 4. TG, DTG, and DTA plots for [Cu(HPPK)(PPK)Cl] · H_2O (*I*) registered in air (a) and in nitrogen (b).

the corresponding pyridyl rings, similar to angles observed in *I*–*III*. All aromatic rings are flat within the maximal root-mean-square deviation of 0.010 Å. Due to the deprotonation of the O3 oxygen atom, there is no possibility for intramolecular hydrogen bonding. The O1 atom bridges with the copper ions in the dimer leading to the closest intermetallic distance of 3.556 Å.

Hence comparing *I* to *IV*, there are subtle changes in the geometry of the oxime group, which depend on its binding character. The shortest N—O distance was observed in the free PPK anion in *IV*. Bridging N—O bonds in *IV* are slightly longer when the oxygen atoms are directly coordinated. The longest N—O bonds were found in the N—O—H groups in *II* and *III*. Distances for C—N bonds in the oxime group revealed an opposite trend: the longest are the C—N bonds in the free PPK anion in the dimer structure of *IV*, whereas the shortest are those in the protonated group. Hence, the protonation of oxygen has the most pronounced effect on the geometry of the oxime group itself.

Thermal studies

Results of thermal analysis performed in air are presented in Table 2. Decomposition of *I* proceeds in four stages with the total mass loss of approximately 84.5 % (Fig. 4). Characterization by powder X-ray diffraction demonstrates the formation of CuO as the final product. TG-IR results for the evolved gases sampled during the decomposition of *I* indicate low intensity bands from CO_2 (2360 cm^{-1}) and C≡C or/and C≡N bond stretching vibrations. After 50 min of heating ($T > 500$ °C), the intensity of carbon dioxide bands in the IR spectrum of the evolved gases products increased notably and an additional

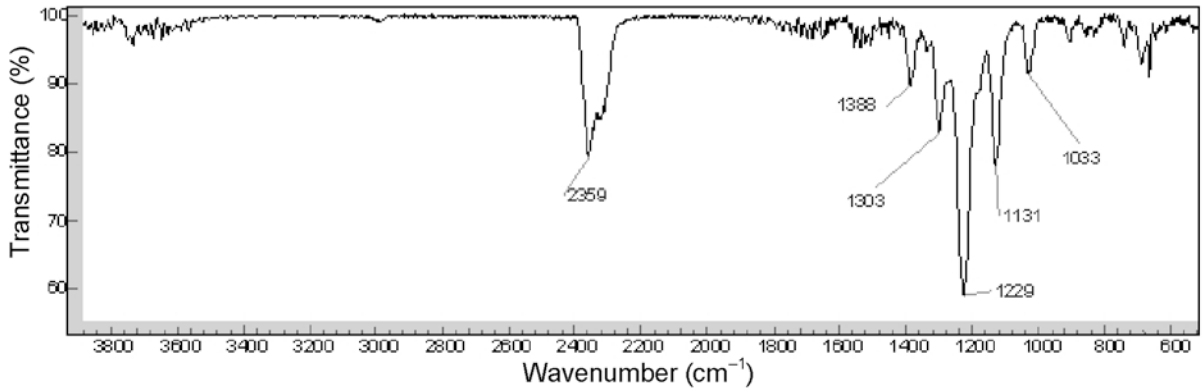

Fig. 5. FT-IR spectrum of volatile products evolved during thermal decomposition of [Cu(HPPK)(PPK)(C_3F_7COO)] (*III*) at 190 °C in air.

Table 3. Results of the thermal analysis of *I*–*IV* in nitrogen atmosphere (10 °C min^{-1})

Compound	Heat effect on DTA	Temperature[a] (°C)			Mass loss (%)	
		T_i	T_m	T_f	Calc. (for Cu formation)	Found
I	endo	58	115	160	87.6	87.6
	exo	160	172	–		
	endo	–	196	–		
	exo	–	777	1000		
II	exo	155	194	–	88.9	82.9
		–	223	–		
		–	228	–		
		–	234	1000		
III		150	164	–	90.5	87.9
	exo	–	170	–		
	exo	–	180	–		
	exo	–	182	–		
	exo	–	206	–		
		–	302	1000		
IV	endo	25	55	63	87.1	83.5
	exo	161	191	204		
	exo	223	243	–		
	exo	–	365	1000		

a) T_i, T_m, and T_f represent initial, at peak maximum, and final temperature, respectively.

band at 3736 cm^{-1} appeared (attributable to ν(NH) or ν(OH)).

Complex *II* is thermally stable up to 168 °C. Above this temperature, in the range of 205–265 °C, the first gaseous products of thermolysis are observed. IR of the gases revealed strong bands derived from ν(C—F) and CO_2. Above 265 °C, only carbon dioxide was registered in the IR spectra. A similar composition of gaseous products was observed for *III* (Fig. 5).

The TG curve for *IV* shows five processes up to 1000 °C and a total mass loss higher than that calculated for the oxidation to CuO. Such increased mass loss may be explained by the displacement of material from the sample pan following the rapid release of gases. Partial dehydration (even at temperatures below 30 °C) might account for the discrepancy between the elemental analysis results and the crystallographic chemical composition. The IR spectra revealed only the presence of CO_2 in the evolved gas stream.

Analogous measurements were performed in nitrogen atmosphere resulting in results similar to those performed in air (Table 3). The primary differences can be observed at higher temperatures, where strong exothermic processes occur at above 400 °C in air (Fig. 4) and no such events can be seen in nitrogen atmosphere. In fact, in nitrogen atmosphere, a continuous mass loss takes place up to 1000 °C suggesting copper formation, which was confirmed by powder XRD data collected for the resulting TGA products.

Volatile species from the thermolysis of *I* in nitrogen were observed above 600 °C. IR spectra revealed broad bands at 3423 cm^{-1} (ν(NH) or ν(OH)),

2360 cm^{-1} (CO_2), and 1650 cm^{-1} (ν(C═N) or ν(C═O)) confirming HPPK decomposition as discussed below. IR spectrum of the gaseous products for *II* revealed three peaks. Bands at 1151 cm^{-1} (vs, sharp, ν(CF)), 1376 cm^{-1}, 3035 cm^{-1}, and from CO_2 (2359 cm^{-1}) were observed in the temperature range of 190–270 ℃. Carbon dioxide was the sole volatile product observed between 310–370 ℃ and 400–500 ℃. Composition of the volatile products of complex *III* was analogous to that of *II*. No peaks besides those derived from CO_2 and H_2O were noted in the thermal decomposition of *IV*.

Studies of copper(II) complexes formed with pyridine-2-aldoxime (Bucci et al., 1984) revealed a similar trend in their thermal behavior as in the complexes studied here. Initial temperature of decomposition was lower for the dimeric compound *IV* than for *I*. In both cases, decomposition of the complexes in the presence of oxygen resulted in sample mass stabilization and reaction completion at lower temperatures than in nitrogen atmosphere (below 700 ℃ for ketoxime complexes) with the same final product (CuO). Thermal decomposition of various types of copper(II) complexes in air frequently results in the formation of copper(II) oxide but the final products of the equivalent thermolysis in nitrogen can be dramatically different (e.g., Cu, CuO, Cu_2O, CuS) depending on the composition of the ligand and on the mechanism of the decomposition process (Sceney et al., 1975; Prasad, 2003; Nasui et al., 2011).

In summary, thermal decomposition reactions of *I*–*IV* occur in two discrete steps. The first step involves partial HPPK ligand decomposition and anion detachment. At higher temperatures, the HPPK aromatic rings are completely decomposed but in gaseous nitrogen, additional reduction to copper(0) occurs. Hence single-phase semiconducting materials cannot be obtained under these conditions. This copper(II) to copper(0) reduction is characterized by slow mass loss up to 1000 ℃, which is evident especially in the complexes with carboxylates, where IR spectra clearly demonstrate the presence of C—F vibrations in the first stage of thermolysis. At higher temperatures, increased amounts of CO_2 and H_2O are detected as a result of aromatic hydrocarbon decomposition.

Ammonolysis reactions

Complexes *II* and *IV* were chosen for preliminary ammonolysis experiments. Products were analyzed by IR, SEM/EDX, and X-ray powder diffraction. Solids obtained after the treatment with ammonia indicated the presence of C≡N or C≡C bonds (about 2200 cm^{-1}), C—H (2850–2930 cm^{-1}), and C═N bonds (approximately 1440 cm^{-1}) under these conditions. In addition, there was no indication of bands originating from Cu—N vibrations in the spectra which should occur at about 650 cm^{-1} (Singh, 1971). EDX spectra showed, in some cases, an increase in the nitrogen content in relation to the starting compound. Moreover, a decrease in the carbon content was observed. Simultaneously, X-ray patterns clearly proved the formation of metallic copper.

Preliminary results indicate that *II* and *IV* are not good precursors for Cu_3N preparation under the considered conditions. According to literature reports, the reaction of gaseous ammonia with e.g. CuF_2 at temperatures above 300 ℃ results in single-phase Cu_3N (Juza & Rabenau, 1956; Juza & Hahn, 1939; Paniconi et al., 2007). The inability to obtain such a product in the presented experiments can be caused by the relatively high carbon content in the final products, which could in turn instigate the carbothermal reduction of copper(II) to copper(0) according to the reactions:

$$2CuO_{(s)} + C_{(s)} \rightarrow 2Cu_{(s)} + CO_{2(g)} \quad (1)$$

or

$$CuO_{(s)} + C_{(s)} \rightarrow Cu_{(s)} + CO_{(g)} \quad (2)$$

Spin coating experiments

A mixture of methanol and acetonitrile was chosen for the spin-coating experiments due to the good solubility of complex *II* in this mixture. The film quality was highly dependent on the spin rate. In general, higher spin speeds and longer spin times result in thinner films. Reducing the drying rate increases the film uniformity. Slight variations in the coating parameters can also result in drastic changes in the film topography.

Optical microscopy demonstrated a broad range of the size of the deposited crystallites and low uniformity of the surface coverage at 1000 min^{-1}. Increased number of molecular precursor species at the substrate surface can be expected at the speed increased to 3000 min^{-1}. This is reflected in the increased substrate coverage at 3000 min^{-1} and 5000 min^{-1}. The complex is deposited as separated grains or/and islands of microcrystals and hence the coating layers are discontinuous. The largest crystals are a few microns in size.

Unpopulated areas between the crystals deposited on the substrate visible under an optical microscope were analyzed in greater detail by AFM (Figs. 6a and 6b) and variations in the spin parameters have been proved to have significant effects on the surface topology. Some samples essentially comprised scattered particles 1–0.4 μm in diameter with heights of 20–100 nm or 200–400 nm with 5–15 nm.

According to thermal analysis and XRD studies of the bulk materials, heating complexes in air results in single-phase copper(II) oxide. Films of *IV* heated in air produce smoother but still not uniform layers consisting principally of grains of 100–200 nm in diameter, although larger particles (about 500 nm) are also

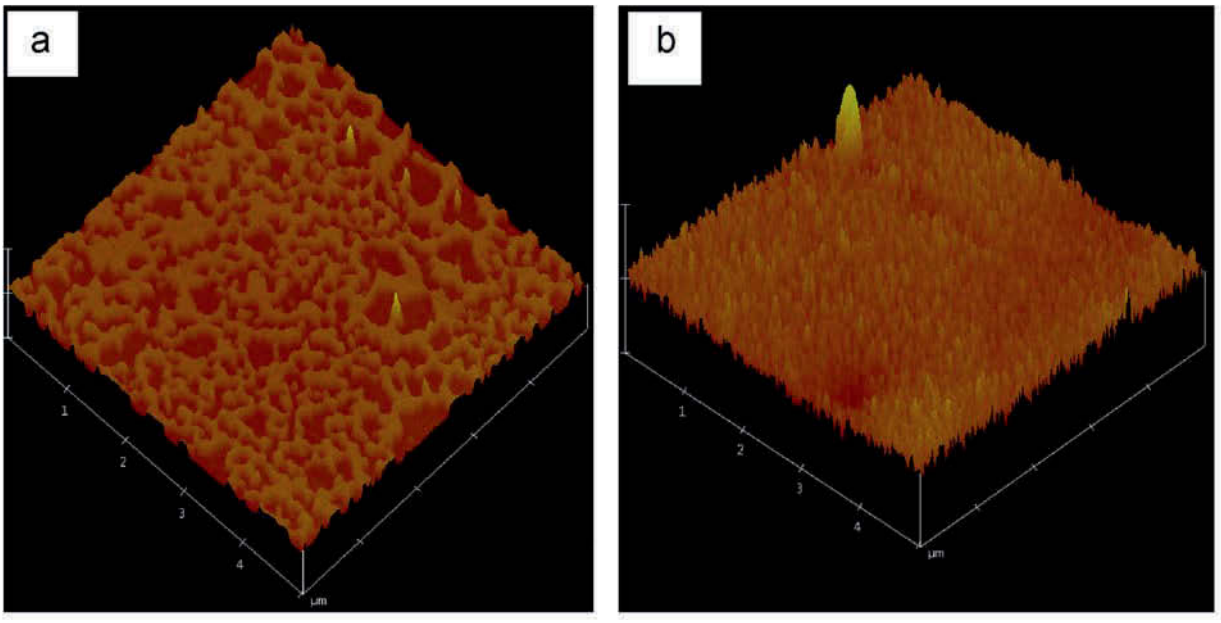

Fig. 6. AFM images of films of *IV*: deposited on Si at 3000 min^{-1}, 60 s (a); after deposition at 3000 min^{-1}, 120 s, and after heating in air (b). (Units are in micrometers on each axis.)

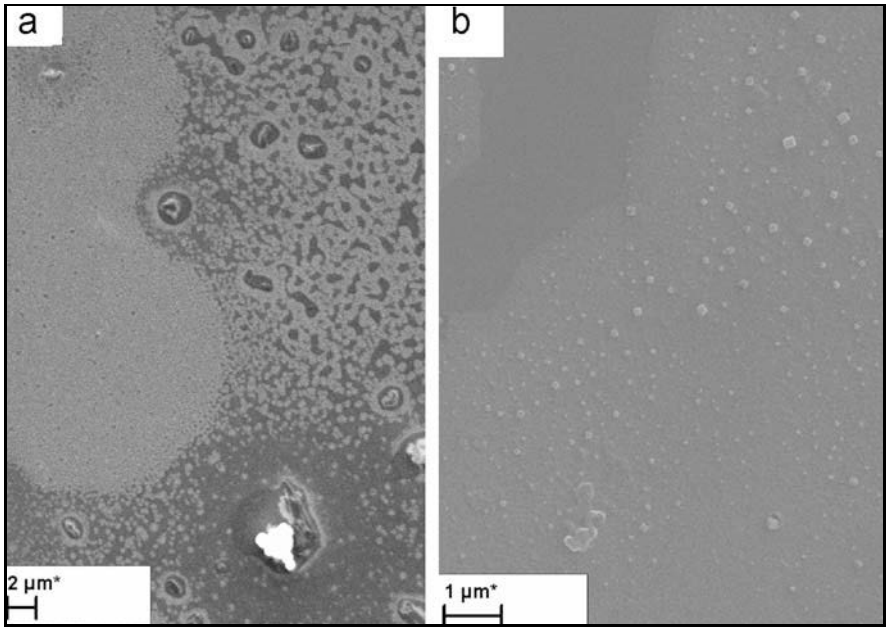

Fig. 7. SEM micrographs of films of *IV*: deposited on Si at 3000 min^{-1} (a), 60 s; after deposition at 3000 min^{-1}, 120 s, and after heating in air (b).

present (Fig. 6b). Morphology of the films was also characterized by scanning electron microscopy (SEM) before (Fig. 7a) and after annealing (Fig. 7b). In these figures, the as-deposited film (Fig. 7a) shows an island-like distribution on the substrate with a rough surface and a clearly non-uniform deposition. After annealing at 800 ℃ in air, the film becomes much more homogeneous but it is still not completely uniform (Fig. 7b).

Deposition and annealing experiments thus suggest that Cu(II)–HPPK complexes are promising precursors to thin films, but further investigation is clearly required. In our future studies, processing methods to improve the homogeneity of these films will be developed and the subsequent analysis is expected to improve our understanding of the nanostructure control.

Conclusions

Two novel (*II* and *III*) and two previously known (*I* and *IV*) copper(II) phenyl-2-pyridylketoxime com-

plexes were prepared. Single crystal X-ray diffraction revealed that *I–IV* contain Cu(II) ions in slightly distorted square pyramidal environments. In all cases, phenyl-2-pyridylketoxime molecules acted as chelating ligands in the base of the square pyramids. TG-IR data revealed that the studied compounds decompose and oxidize in air below 700 ℃ but the decomposition continues up to 1000 ℃ in nitrogen atmosphere. Annealing in ammonia atmosphere at 450 ℃ led to the decomposition and reduction of copper(II) to copper(0), visible in the XRD pattern as a copper metal.

The potential of the complexes to serve as precursors to copper containing materials in spin coating was also investigated. Preliminary results are promising in that CuO films can be prepared using this route. However, the coating parameters improving the uniformity of the cover should be identified using TG-DTA to enable the preparation of metal oxide films following these procedures.

Acknowledgements. The study was supported by a Research Fellowship for R. S. within the project "Enhancing the Educational Potential of Nicolaus Copernicus University in the Disciplines of Mathematical and Natural Sciences" (project no. POKL.04.01.01-00-081/10.). The authors would also like to thank the Polish National Science Center (NCN) for financial support (grant no. 21889, UMO-2013/09/B/ST5/03509).

Supplementary data

Supplementary data associated with this article can be found in the online version of this paper (DOI: 10.1515/chempap-2015-0065).

References

Addison, A. W., Rao, T. N., Reedijk, J., van Rijn, J., & Verschoor, G. C. (1984). Synthesis, structure, and spectroscopic properties of copper(II) compounds containing nitrogen–sulphur donor ligands; the crystal and molecular structure of aqua[1,7-bis(*N*-methylbenzimidazol-2′-yl)-2,6-dithiaheptane]copper(II) perchlorate. *Journal of the Chemical Society, Dalton Transactions*, *1984*, 1349–1356. DOI: 10.1039/dt9840001349.

Afrati, T., Dendrinou-Samara, C., Raptopoulou, C., Terzis, A., Tangoulis, V., & Kessissoglou, D. P. (2007). Copper inverse-9-metallacrown-3 compounds showing antisymmetric magnetic behaviour. *Dalton Transactions*, *2007*, 5156–5164. DOI: 10.1039/b708767e.

Afrati, T., Pantazaki, A. A., Dendrinou-Samara, C., Raptopoulou, C., Terzis, A., & Kessissoglou, D. P. (2010). Copper inverse-9-metallacrown-3 compounds interacting with DNA. *Dalton Transactions*, *39*, 765–775. DOI: 10.1039/b914112j.

Ando, M., Kobayashi, T., Iijima, S., & Haruta, M. (2003). Optical CO sensitivity of Au–CuO composite film by use of the plasmon absorption change. *Sensors and Actuators B: Chemical*, *96*, 589–595. DOI: 10.1016/s0925-4005(03)00645-2.

Baker, P. G. L., Sanderson, R. D., & Crouch, A. M. (2007). Sol–gel preparation and characterisation of mixed metal tin oxide thin films. *Thin Solid Films*, *515*, 6691–6697. DOI: 10.1016/j.tsf.2007.01.042.

Barreca, D., Gasparotto, A., Maccato, C., Tondello, E., Lebedev, O. I., & Van Tendeloo, G. (2009). CVD of copper oxides from a β-diketonate diamine precursor: tailoring the nanoorganization. *Crystal Growth & Design*, *9*, 2470–2480. DOI: 10.1021/cg801378x.

Bayansal, F., Çetinkara, H. A., Kahraman, S., Çakmak, H. M., & Güder, H. S. (2012). Nano-structured CuO films prepared by simple solution methods: Plate-like, needle-like and network-like architectures. *Ceramics International*, *38*, 1859–1866. DOI: 10.1016/j.ceramint.2011.10.011.

Brandenburg, K. (2001). Diamond, Release 2.1e [computer software]. Bonn, Germany: Crystal Impact.

Bräuer, B., Zahn, D. R. T., Rüffer, T., & Salvan, G. (2006). Deposition of thin films of a transition metal complex by spin coating. *Chemical Physics Letters*, *432*, 226–229. DOI: 10.1016/j.cplett.2006.10.070.

Bucci, R., Carunchio, V., Magri, A. D., & Magri, A. L. (1984). The thermal decomposition reactions of bis-(pyridine-2-aldoxime)-copper(II) complexes. *Journal of Thermal Analysis and Calorimetry*, *29*, 679–686. DOI: 10.1007/bf01913525.

Chakravorty, A. (1974). Structural chemistry of transition metal complexes of oximes. *Coordination Chemistry Reviews*, *13*, 1–46. DOI: 10.1016/s0010-8545(00)80250-7.

Oxford Diffraction (2000). CrysAlis RED and CrysAlis CCD [computer software]. Abingdon, UK: Oxford Diffraction.

Elschner A., Heuer, H. W., Jonas, F., Kirchmeyer, S., Wehrmann, R., & Wussow, K. (2001). Gallium complexes in three-layer organic electroluminescent devices. *Advanced Materials*, *13*, 1811–1814. DOI: 10.1002/1521-4095(200112)13:23<1811::AID-ADMA1811>3.0.CO;2-G.

Farrugia, L. J. (1997). *ORTEP*-3 for Windows – a version of *ORTEP*-III with a Graphical User Interface (GUI). *Journal of Applied Crystallography*, *30*, 565. DOI: 10.1107/s0021889897003117.

Hall, D. B., Underhill, P., & Torkelson, J. M. (1998). Spin coating of thin and ultrathin polymer films. *Polymer Engineering & Science*, *38*, 2039–2045. DOI: 10.1002/pen.10373.

Hudák, A., & Košturiak, A. (1999). Preparation, IR characterization and thermal properties of some metal complexes of isatin-3-oxime. *Journal of Thermal Analysis and Calorimetry*, *58*, 579–587. DOI: 10.1023/a:1010148310379.

Huh, P. H., Yang, J. Y., & Kim, S. C. (2012). Facile formation of nanostructured 1D and 2D arrays of CuO islands. *RSC Advances*, *2*, 5491–5494. DOI: 10.1039/c2ra20097j.

Ji, Z. G., Yuan, Y. H., Yuan, Y., & Wang, C. (2006). Reactive DC magnetron deposition of copper nitride films for write-once optical recording. *Materials Letters*, *60*, 3758–3760. DOI: 10.1016/j.matlet.2006.03.107.

Juza, R., & Hahn, H. (1939). Kupfernitrid Metallamide und Metallnitride. VII. *Zeitschrift für Anorganische und Allgemeine Chemie*, *241*, 172–178. DOI: 10.1002/zaac.19392410204. (in German)

Juza, R., & Rabenau, A. (1956). Das elektrische Leitvermögen einiger Metallnitride. *Zeitschrift für Anorganische und Allgemeine Chemie*, *285*, 212–220. DOI: 10.1002/zaac.19562850314. (in German)

Kida, T., Oka, T., Nagano, M., Ishiwata, Y., & Zheng, X. G. (2007). Synthesis and application of stable copper oxide nanoparticle suspensions for nanoparticulate film fabrication. *Journal of the American Ceramic Society*, *90*, 107–110. DOI: 10.1111/j.1551-2916.2006.01402.x.

Kim, S. G., Hagura, N., Iskandar, F., Yabuki, A., & Okuyama, K. (2008). Multilayer film deposition of Ag and SiO_2 nanoparticles using a spin coating process. *Thin Solid Films*, *516*, 8721–8725. DOI: 10.1016/j.tsf.2008.05.053.

Koumousi, E. S., Raptopoulou, C. P., Perlepes, S. P., Escuer, A., & Stamatatos, T. C. (2010). Strong antiferromagnetic coupling in doubly *N,O* oximato-bridged dinu-

clear copper(II) complexes. *Polyhedron*, *29*, 204–211. DOI: 10.1016/j.poly.2009.07.010.

Li, Q., Mei, P., & Xiang, J. (2006). Di-μ-chloro-bis[chloro (phenyl 2-pyridyl ketone oxime-κ^2N, N')copper(II)]. *Acta Crystallographica Section E*, *62*, m2348–m2349. DOI: 10.1107/s1600536806033836.

Liu, C. H., & Liu, C. F. (1961). Hetero-binuclear chelates of copper(II) and silver(I). *Journal of the American Chemical Society*, *83*, 4167–4169. DOI: 10.1021/ja01481a015.

Liu, G. X., Yang, H., Nishihara, S., & Ren, X. M. (2010). A trinuclear Cu(II) complex from the use of phenyl 2-pyridyl ketoxime: Structure and magnetic behavior. *Synthesis and Reactivity in Inorganic, Metal-Organic, and Nano-Metal Chemistry*, *40*, 421–424. DOI: 10.1080/15533174.2010.492557.

Meek, T. L., & Cheney, G. E. (1965). The copper(II) *syn*-phenyl-2-pyridyl ketoxime system. Part I. *Canadian Journal of Chemistry*, *43*, 64–74. DOI: 10.1139/v65-009.

Milios, C. J., Kefalloniti, E., Raptopoulou, C. P., Terzis, A., Escuer, A., Vicente, R., & Perlepes, S. P. (2004). 2-Pyridinealdoxime [(py)CHNOH] in manganese(II) carboxylate chemistry: mononuclear, dinuclear, tetranuclear and polymeric complexes, and partial transformation of (py)CHNOH to picolinate(–1). *Polyhedron*, *23*, 83–95. DOI: 10.1016/j.poly.2003.09.009.

Milios, C. J., Stamatatos, T. C., & Perlepes, S. P. (2006). The coordination chemistry of pyridyl oximes. *Polyhedron*, *25*, 134–194. DOI: 10.1016/j.poly.2005.07.022.

Mohan, M., & Paramhans, B. D. (1980). Transition metal chemistry of oxime-containing ligands, part XI. Copper(II) complexes of syn-phenyl-2-pyridylketoxime and syn-methyl-2-pyridylketoxime. *Transition Metal Chemistry*, *5*, 113–117. DOI: 10.1007/bf01396885.

Nasui, M., Mos, R. B., Petrisor, T., Jr., Gabor, M. S., Varga, R. A., Ciontea, L., & Petrisor, T. (2011). Synthesis, crystal structure and thermal decomposition of a new copper propionate $[Cu(CH_3CH_2COO)_2] \cdot 2H_2O$. *Journal of Analytical and Applied Pyrolysis*, *92*, 439–444. DOI: 10.1016/j.jaap.2011.08.005.

Navío, C., Alvarez, J., Capitan, M. J., Camarero, J., & Miranda, R. (2009). Thermal stability of Cu and Fe nitrides and their applications for writing locally spin valves. *Applied Physics Letters*, *94*, 263112. DOI: 10.1063/1.3159630.

Paniconi, G., Stoeva, Z., Doberstein, H., Smith, R. I., Gallagher, B. L., & Gregory, D. H. (2007). Structural chemistry of Cu_3N powders obtained by ammonolysis reactions. *Solid State Sciences*, *9*, 907–913. DOI: 10.1016/j.solidstatesciences.2007.03.017.

Partridge, A., Toussaint, S. L. G., & Flipse, C. F. J. (1996). An AFM investigation of the deposition of nanometer-sized rhodium and copper clusters by spin coating. *Applied Surface Science*, *103*, 127–140. DOI: 10.1016/0169-4332(96)00520-x.

Prasad, R. (2003). Mechanism and kinetics of thermal decomposition of ammoniacal complex of copper oxalate. *Thermochimica Acta*, *406*, 99–104. DOI: 10.1016/s0040-6031(03)00225-9.

Prathapachandra Kurup, M. R., Chandra, S. V., & Muraleedharan, K. (2000). Synthesis, spectral and thermal studies of *o*-vanillin oxime complexes of zinc(II), cadmium(II) and mercury(II). *Journal of Thermal Analysis and Calorimetry*, *61*, 909–914. DOI: 10.1023/a:1010154810885.

Salonen, M., Saarinen, H., & Orama, M. (2003). Formation of zinc(II) and cadmium(II) complexes with pyridine oxime ligands in aqueous solution. *Journal of Coordination Chemistry*, *56*, 1041–1047. DOI: 10.1080/00958970310001596737.

Sathaye, S. D., Patil, K. R., Kulkarni, S. D., Bakre, P. P., Pradhan, S. D., Sarwade, B. D., & Shintre, S. N. (2003). Modification of spin coating method and its application to grow thin films of cobalt ferrite. *Journal of Materials Science*, *38*, 29–33. DOI: 10.1023/a:1021101529855.

Sceney, C. G., Hill, J. O., & Magee, R. J. (1975). Thermal analysis of copper dithiocarbamates. *Thermochimica Acta*, *11*, 301–306. DOI: 10.1016/0040-6031(75)85099-4.

Schubert, D. W., & Dunkel, T. (2003). Spin coating from a molecular point of view: its concentration regimes, influence of molar mass and distribution. *Materials Research Innovations*, *7*, 314–321. DOI: 10.1007/s10019-003-0270-2.

Sheldrick, G. M. (2008). A short history of *SHELX*. *Acta Crystallographica Section A*, *64*, 112–122. DOI: 10.1107/s0108767307043930.

Singh, K. (1971). Magnetic and spectroscopic studies on cupric azide. *Transactions of the Faraday Society*, *67*, 2436–2444. DOI: 10.1039/tf9716702436.

Wang, J., Chen, J. T., Yuan, X. M., Wu, Z. G., Miao, B. B., & Yan, P. X. (2006). Copper nitride (Cu_3N) thin films deposited by RF magnetron sputtering. *Journal of Crystal Growth*, *286*, 407–412. DOI: 10.1016/j.jcrysgro.2005.10.107.